Modulation of Proteome Profile in AβPP/PS1 Mice Hippocampus, Medial Prefrontal Cortex, and Striatum by Palm Oil Derived Tocotrienol-Rich Fraction

Hamizah Shahirah Hamezah[a], Lina Wati Durani[a], Daijiro Yanagisawa[a], Nor Faeizah Ibrahim[b],
Wan Mohd Aizat[c], Suzana Makpol[b], Wan Zurinah Wan Ngah[b], Hanafi Ahmad Damanhuri[b]
and Ikuo Tooyama[a,*]

[a]*Molecular Neuroscience Research Center, Shiga University of Medical Science, Seta Tsukinowa-cho,
Otsu, Japan*
[b]*Department of Biochemistry, Faculty of Medicine, UKMMC, Universiti Kebangsaan Malaysia (UKM),
Jalan Yaacob Latif, Cheras, Kuala Lumpur, Malaysia*
[c]*Institute of Systems Biology, Universiti Kebangsaan Malaysia, Bangi, Selangor, Malaysia*

Abstract. Tocotrienol-rich fraction (TRF) is a mixture of vitamin E analogs derived from palm oil. We previously demonstrated that supplementation with TRF improved cognitive function and modulated amyloid pathology in AβPP/PS1 mice brains. The current study was designed to examine proteomic profiles underlying the therapeutic effect of TRF in the brain. Proteomic analyses were performed on samples of hippocampus, medial prefrontal cortex (mPFC), and striatum using liquid chromatography coupled to Q Exactive HF Orbitrap mass spectrometry. From these analyses, we profiled a total of 5,847 proteins of which 155 proteins were differentially expressed between AβPP/PS1 and wild-type mice. TRF supplementation of these mice altered the expression of 255 proteins in the hippocampus, mPFC, and striatum. TRF also negatively modulated the expression of amyloid beta A4 protein and receptor-type tyrosine-protein phosphatase alpha protein in the hippocampus. The expression of proteins in metabolic pathways, oxidative phosphorylation, and those involved in Alzheimer's disease were altered in the brains of AβPP/PS1 mice that received TRF supplementation.

Keywords: Alzheimer's disease, LC-MS, palm oil, proteomics, tocotrienol

INTRODUCTION

Alzheimer's disease (AD) is the most common form of dementia, which is characterized by a progressive decline in memory and cognitive capabilities, accompanied by neuropathological hallmarks, such as aggregates of amyloid-β (Aβ) in plaques and neurofibrillary tangles [1]. Aβ is generated from sequential proteolytic processing of amyloid-β protein precursor (AβPP) by β- and γ-secretases [2]. The progression of AD can be influenced by genetic, environment, and lifestyle factors [3]. AD commonly occurs with advanced age, but it may also have an early-onset, as observed with familial AD through the enhanced generation and accumulation of Aβ caused by mutations in *APP* or presenilins-1 and 2 (*PSEN1* and *PSEN2*) [4, 5]. Overall, it is important

*Correspondence to: Ikuo Tooyama, MD, PhD, Molecular Neuroscience Research Center, Shiga University of Medical Science, Seta Tsukinowa-cho, Otsu 520-2192, Japan. Tel.: +81 77 548 2330; Fax: +81 77 548 2331; E-mail: kinchan@belle.shiga-med.ac.jp.

to find a cure for AD at an early preclinical stage, and various natural-source compounds are one possible therapeutic approach.

Vitamin E, a lipid soluble vitamin, has been shown to preserve cognitive function and general well-being in the elderly [6–8]. However, a previous randomized controlled trial has reported that vitamin E in the form of α-tocopherol showed no significant effects on AD progression compared to the placebo group [9], while Dysken et al. showed that α-tocopherol was effective in slowing the progression of mild to moderate AD [6]. Vitamin E in the form of tocotrienols exhibits a significantly greater neuroprotective effect than α-tocopherol as it has been shown to protect against glutamate-induced neuronal death by suppressing inducible pp60 c-Src kinase activation at a nanomolar concentration [10]. Vitamin E is composed of tocopherols and tocotrienols. Tocopherols and tocotrienols have isomers, designated as α-, β-, γ-, and δ-, which differ by the number and position of methyl groups on the chromanol ring [11]. Tocotrienols differ from tocopherols by the presence of three double bonds in their isoprenoid side chain, which contributes to easier penetration into saturated fatty acid layers around the brain, thereby providing higher efficacy and potency as antioxidants [12, 13]. The combination of tocotrienols and tocopherols has been shown to be neuroprotective and to reduce AD risk at an advanced age [14].

A major source of vitamin E containing nearly 70% tocotrienols and 30% tocopherols is palm oil from *Elais guineensis* (African oil palm tree) [15, 16]. Tocotrienol-rich fraction (TRF), a mixture of vitamin E analogs derived from palm oil, has garnered attention recently. Several reports have shown the potential of TRF in modulating Aβ metabolism [17], brain metabolites [18, 19], antioxidant defense mechanisms [19, 20], and cancer prevention [21]. Previously we have demonstrated that long-term supplementation (ten months) of TRF on APPswe/PS1dE9 double transgenic (Tg) mice (AβPP/PS1), a mouse model of AD, reduced amyloid pathology in the brain [17]. Long-term supplementation of TRF has also been shown to enhance spatial memory, working memory, and locomotor activity of AβPP/PS1 mice [18]. Our recent metabolomics study showed that TRF exerts its neuroprotective effect in the AβPP/PS1 mice brain possibly by modulating metabolic pathways involved in bioenergetics, neurotransmission, membrane lipid metabolism, and oxidative stress defense [18]. However, the effect of TRF on AβPP/PS1 mice has not yet been investi-

gated at the proteome level. This is essential to further understand the progression of AD-like pathogenesis in AβPP/PS1 mice, and how TRF might be altering the onset and progression of the disease.

Hence, the present study examined the proteome profile of AβPP/PS1 mice hippocampus, medial prefrontal cortex (mPFC), and striatum, compared to wild-type (WT) mice. In addition, we also analyzed the effect of TRF supplementation on these brain regions of AβPP/PS1 mice, by comparing them with its vehicle control group, Tg-PO mice, which received palm oil stripped of vitamin E. To our knowledge, this is the first study analyzing the effect of TRF on untargeted proteome profile of AβPP/PS1 mice brain regions (hippocampus, mPFC, and striatum) by using ultrahigh-performance liquid chromatography (UHPLC) coupled to Q Exactive HF Orbitrap mass spectrometry.

MATERIALS AND METHODS

Animals

APPswe/PS1dE9 double transgenic (Tg) mice (AβPP/PS1) line 85, expressing a chimeric mouse/ human amyloid precursor protein (Mo/HuAPP695 swe) and a mutant human presenilin 1 with deletion at exon-9 (PS1-dE9), were obtained from Jackson Laboratory (Bar Harbor, ME, USA) [22]. Mice were maintained by breeding heterozygous females with WT males. The offspring were genotyped by polymerase chain reaction (PCR) using the APP primers:

forward-GACTGACCACTCGACCAGGTTCTG

/reverse-CTTGTAAGTTGGATTCTCATATCCG,

and the following two presenilins 1 sequences:

forward-CTCTTTGTGACTATGTGGACTGAT GTCGG

/reverse- GTGGATAACCCCTCCCCCAGCC TAGACC

and forward- ATTAGAGAACGGCAGGAGCA

/reverse-GCCATGAGGGCACTAATCAT.

Only heterozygous and WT male mice were used in this study. All mice were housed in a controlled environment (23°C, 12 h/12 h light/dark cycle (lights on from 8:00–20:00)) with *ad libitum* access to food and water. All animal protocols were approved by the Animal Care and Use Committee of the Shiga

University of Medical Science (Ethical committee approval number: 2013-6-12H).

TRF supplementation

The TRF used in this study (Sime Darby, Selangor, Malaysia) consisted of a mixture of α-tocopherol (168.0 mg/g), α-tocotrienol (196.0 mg/g), β-tocotrienol (24.0 mg/g), γ-tocotrienol (255.0 mg/g), and δ-tocotrienol (75.0 mg/g). Palm oil stripped of vitamin E (PO) was purchased from the Malaysian Palm Oil Board (Selangor, Malaysia). TRF was dissolved at 12 mg/mL in PO as previously described [17]. Five-month-old mice were divided into four groups ($n = 3$ per group): two groups received water (WT-ctrl and Tg-ctrl, 5 mL/kg body weight), one group received PO as a vehicle (Tg-PO, 5 mL/kg body weight), and the other received TRF (60 mg/kg body weight). All mice received daily supplementation of TRF (Tg-TRF), PO (Tg-PO), or water (Tg-ctrl and WT-ctrl) by oral gavage for a duration of 10 months. The mice used in the study were subjected to behavioral tests (open field, novel object recognition, and Morris water maze) as reported in our previous study [18].

Proteome analysis in mice brain

Brain tissue preparation

The mice were sacrificed by cervical dislocation. Each brain was rapidly removed and rinsed in ice-cold 10 mM phosphate buffered saline. The brain was sectioned into 1.0 mm coronal slices using a Mouse Brain Slicer Matrix (Zivic Instruments Inc., Pittsburgh, PA, USA), and further dissected into three different regions, hippocampus, mPFC, and striatum, on an ice-cold plate. Each sample was transferred into individual tubes, immediately weighed, frozen on dry ice, and stored at –80°C until analysis.

Protein extraction, protein separation, and in-gel digestion

Protein extraction, protein separation, and in-gel digestion were conducted according to our previously described method [23]. For the protein extraction procedure, the mice hippocampus, mPFC, and striatum were homogenized using an ultrasonicator (QSonica, Newtown, CT, USA). Next, the brain homogenates were centrifuged (20,600 × g, 4°C, 15 min) and the supernatants were collected. Thiourea rehydration buffer was added to the remaining pellets. The mixture was centrifuged (20,600 × g, 4°C, 15 min). The

resulting supernatants were then pooled with the earlier collected supernatants. The protein concentration in each sample was quantified using a Bio-Rad Bradford protein assay kit (Bio-Rad, CA, USA). Each sample containing 50 μg of extracted protein was separated by gel electrophoresis at 120 V constant current. The gel was stained with Simply Blue Safe Stain (Invitrogen, USA) and washed thoroughly to remove excess stain. For in-gel digestion procedure, the gel was cut into six fractions, and further sliced into 1 to 2 mm pieces. Next, the gel pieces were transferred into a tube containing 50% acetonitrile/50 mM ammonium bicarbonate solution and shaken for 15 min. The solution was removed and the process was repeated until no visible stain was observed in the gel pieces. The gel pieces were reduced with 10 mM dithiothreitol/100 mM ammonium bicarbonate solution, alkylated with 55 mM iodoacetamide/100 mM ammonium bicarbonate solution, dehydrated with acetonitrile solution, and dried in a vacuum concentrator. The gel pieces were then incubated overnight with 6 ng of trypsin/50 mM ammonium bicarbonate solution at 37°C. After overnight digestion, the gel pieces were agitated constantly for 15 min in acetonitrile solution. The solution was then transferred into a new tube. The gel pieces were extracted again with 50% acetonitrile/50 mM ammonium bicarbonate solution. The solutions collected from both tubes were pooled into one tube and then dried for about 3 h using a vacuum concentrator at 30°C. The dried peptides from each tissue sample were reconstituted in 0.1% formic acid solution before analysis on the liquid chromatography-tandem mass spectrometry (LC-MS/MS) system.

Liquid chromatography and MS/MS analysis

Proteomics analysis was carried out using LC-MS/MS according to the methods described previously [23]. Upon injection of 6 μL of 50 μg extracted sample into the LC-MS/MS system, the sample underwent chromatographic separation in the Dionex Ultimate 3000 UHPLC instrument (Thermo Fisher Scientific, Waltham, MA, USA) through reversed phase PepMap-C18 pre-column with 300 μm inner diameter × 5 mm length, packed with 5 μm particles, and chromatographed on a PepMap RSLC C18 2 μm, 100 Å, 75 μm × 25 cm column (Thermo Fisher Scientific), at 35°C. The sample was separated using a binary gradient mobile phase system with a total running time of 135 min and a constant flow of 300 nL/min as described previously [23]. A Q Exactive HF (Thermo Scientific)

quadrupole-Orbitrap hybrid instrument was used to acquire mass spectra and tandem mass spectra under the control of the manufacturer's XCalibur version 4.0 software. Electrospray ionization was set at positive mode whereas capillary temperature and spray voltage were applied at 275°C and 1.6 kV, respectively. Full-scan mass spectra were acquired from m/z 350 to 1800 with resolution, automatic gain control (AGC) threshold and maximum injection time set to 120000, 3×10^6 and 100 ms, respectively. For data dependent acquisition, the following settings were applied. Only precursors with an assigned monoisotopic m/z and a charge state of 2 to 7 were included for the MS/MS scans. From survey scans, the software chose in real time maximum 20 precursor ions based on intensity and assigned charge state to trigger subsequent MS/MS acquisitions. Maximum injection time was set at 65 ms and isolation window of 0.7 m/z. Higher energy collisional dissociation (HCD) with a normalized collision energy (NCE) was set to 28%. Minimum AGC threshold was set at 5×10^3, intensity threshold was kept at 7.7×10^4 and apex-triggered MS/MS scan was set at 2 to 15 s. Dynamic exclusion duration used was 20 s to avoid repeating MS/MS scan for the same precursor ion.

Data analysis

Protein identification and quantification

The mass spectra data were analyzed by using MaxQuant version 1.5.3.30 (http://www.maxquant.org) using a similar setting as described previously [23]. The data were searched by the built-in Andromeda search engine [24, 25] against *Mus musculus* sequences obtained from the UniProt database (http://www.uniprot.org) accessed on September 2016. Protein identification was filtered using a target-decoy approach with a false discovery rate (FDR) of 1%. Trypsin was set as the digestive enzyme, while missed cleavage by the enzymatic digestion was set at two sites for the protein sequence. Methionine oxidation and protein N-terminal acetylation were selected as the variable modifications, while cysteine carbamidomethylation was chosen as the constant modification. Minimum peptide length and maximum peptide mass were set to seven amino acid residues and 4,600 Da, respectively (to avoid matching too short and too long tryptic peptides to protein sequences). Label-free quantification (LFQ) approach was applied to quantify the protein. The mass spectrometry proteomics data have been deposited to the ProteomeXchange Consortium via the PRIDE [26] partner repository with the dataset identifier PXD011068.

Bioinformatics and statistical analysis

The data acquired from the MaxQuant was further processed using Perseus software (version 1.5.4.1, Max Planck Institute of Biochemistry, Martinsried, Germany) [27]. The analysis was carried out according to our previously described method with some modifications [23]. First, the data were uploaded into the Perseus software, followed by screening of the proteins by removing potential contaminants, identification of protein based on sites only, and identifications from reversed sequences. The protein abundances from LFQ quantifications were log-transformed. If the calculated values were presented as "NaN" (Non-Assigned Number) values, the values were considered as missing values. The log-transformed LFQ intensity values of the proteins were filtered based on the minimum number of valid values in one experimental group. In the present study, the minimum number of valid values was set at 2, which accepted the proteins showing at least two valid values out of three samples in at least one experimental group out of four experimental groups (either Tg-ctrl, WT-ctrl, Tg-TRF, or Tg-PO groups) to be considered for the analysis. The missing values imputation was applied by considering the estimated intensity distribution. Multi-scatter plot and principal component analysis were carried out in order to estimate the variabilities between biological replicates of the brain sample.

To identify the proteins altered in AβPP/PS1 mice, the Tg-ctrl group was compared to the WT-ctrl group using a two-tailed, *t*-test. Similarly, a *t*-test was also used to test the effect of TRF supplementation on AβPP/PS1 mice by comparing Tg-TRF with its vehicle control group, Tg-PO. A protein was considered to be differentially expressed when the difference between groups had a *p*-value of less than 0.05 ($p < 0.05$). Benjamini-Hochberg test was used for the FDR correction method at a cut off value 0.05. However, since a mild change in the expression of the proteins was observed after performing a Benjamini-Hochberg test, we considered the proteins with $p < 0.05$ as significantly altered in this study. Both *p*-value and *q*-value of each protein are listed in the Supplementary Tables 1–4.

Next, in order to identify overlapped proteins between the differentially expressed proteins ($p < 0.05$) in Tg-ctrl versus WT-ctrl groups and Tg-TRF versus Tg-PO groups, we constructed Venn

diagrams online at http://bioinfogp.cnb.csic.es/tools/venny/index.html [28]. Each significantly altered protein ($p < 0.05$) was subjected to pathway search against Kyoto Encyclopedia of Genes and Genomes (KEGG) databases (http://www.genome.jp/kegg/pathway.html) using a pathway enrichment tool, KEGG orthology-based annotation system (KOBAS) version 3.0 (http://kobas.cbi.pku.edu.cn/) [29, 30]. We selected *Mus musculus* library and KEGG database for the pathway search. The hypergeometric test and Fisher's exact test were used for statistical testing in the pathway enrichment analysis and Benjamini-Hochberg was used for the FDR correction method. For each KEGG pathway, a *p*-value was calculated using a hypergeometric test, and a cutoff of 0.05 was applied to identify enriched KEGG pathways. Only the top five pathways with *p*-values less than 0.05 are listed in Tables 2 and 3.

RESULTS

Profiling of differentially expressed proteins in AβPP/PS1 mice brain

We conducted a bioinformatic analysis of the LC-MS/MS data using MaxQuant and Perseus software to investigate alterations in the proteome profile of AβPP/PS1 mice brain supplemented with TRF extracted from palm oil. From these analyses, we identified 5,847 proteins in the hippocampus, mPFC, and striatum of the AβPP/PS1 mice control and WT mice groups (Supplementary Table 1). Meanwhile, 6,047 proteins were identified in the AβPP/PS1 mice in the TRF and PO groups (Supplementary Table 2). Next, we assessed the proteome data quality by comparing the relative protein quantification among the three biological replicates of each group. Multi-scatter plots with Pearson's correlation coefficients were about 0.5–1.0, demonstrating good reproducibility between the biological replicates in each

experimental group: Tg-ctrl and WT-ctrl (Fig. 1A–C), as well as Tg-TRF and Tg-PO (Fig. 1D–F). Principal component analysis also showed that the biological replicates in each group were closely clustered, as visualized by the separation trends between Tg-ctrl and WT-ctrl (Fig. 2A–C), and also between Tg-TRF and Tg-PO (Fig. 2D–F).

To investigate alterations in the proteome profile of AβPP/PS1 mice brains, a comparison was made between the Tg-ctrl versus WT-ctrl groups (Table 1, Supplementary Table 3). A total of 155 proteins were significantly altered ($p < 0.05$) in Tg-ctrl compared with WT-ctrl mice hippocampus, mPFC, and striatum. Analyses of proteome data in these mice groups showed that the levels of 43 proteins were altered ($p < 0.05$) in the hippocampus (26 upregulated and 17 downregulated). The levels of 99 proteins were altered ($p < 0.05$) in mPFC (16 upregulated and 83 downregulated). In the striatum, the levels of 13 proteins were altered ($p < 0.05$), with 12 of them upregulated and 1 downregulated.

Next, we compared the protein levels in Tg-TRF and Tg-PO groups to test the effect of TRF on the AβPP/PS1 mice brain proteome (Table 1, Supplementary Table 4). We found that the levels of 255 proteins were significantly altered ($p < 0.05$) in Tg-TRF compared to Tg-PO mice in all brain regions studied. Of these, 203 proteins levels were altered ($p < 0.05$) in the hippocampus (65 upregulated and 138 downregulated). In the mPFC, a total of 29 proteins levels were altered ($p < 0.05$) with 14 upregulated and 15 downregulated proteins. The levels of 23 proteins were altered ($p < 0.05$) in the striatum of Tg-TRF group compared with Tg-PO with 18 and 5 proteins being upregulated or downregulated, respectively.

Pairwise comparison of the differentially expressed proteins ($p < 0.05$) between Tg-ctrl versus WT-ctrl and Tg-TRF versus Tg-PO was made to investigate the overlapped proteins between these

Table 1

Number of altered proteins between AβPP/PS1 transgenic mice control (Tg-ctrl) compared with wild type mice (WT-ctrl) (Tg-ctrl versus WT-ctrl) and between AβPP/PS1 transgenic mice treated with tocotrienol-rich fraction (Tg-TRF) compared with the vehicle control group, AβPP/PS1 transgenic mice treated with palm oil stripped of vitamin E (Tg-PO) (Tg-TRF versusTg-PO) in mice hippocampus, medial prefrontal cortex, and striatum

Brain region	Hippocampus		Medial prefrontal cortex		Striatum	
Groups	Tg-ctrl versus WT-ctrl	Tg-TRF versus Tg-PO	Tg-ctrl versus WT-ctrl	Tg-TRF versus Tg-PO	Tg-ctrl versus WT-ctrl	Tg-TRF versus Tg-PO
Upregulated	26	65	16	14	12	18
Downregulated	17	138	83	15	1	5
Total	43	203	99	29	13	23

Table 2

Kyoto Encyclopedia of Genes and Genomes (KEGG) pathway enrichment for the differentially expressed proteins from AβPP/PS1 transgenic mice control (Tg-ctrl) compared with wild type mice (WT-ctrl) using KOBAS. The pathways are arranged according to the number of differentially expressed proteins in each pathway. Only the top five enriched pathways ($p < 0.05$) are listed. ↓ represents significantly downregulated ($p < 0.05$) protein. ↑ represents significantly upregulated ($p < 0.05$) protein

Pathway	Proteins number	p	Corrected p	Accession number	Protein names	Gene names	Proteins expression
Hippocampus							
Alzheimer's disease	3	0.0073	0.2502	P12023	Amyloid beta A4 protein	APP	↑
				Q63810	Calcineurin subunit B type 1	PPP3R1	↑
				Q9D0M3	Cytochrome c1	CYC1	↓
Glutamatergic synapse	3	0.003	0.2064	Q63810	Calcineurin subunit B type 1	PPP3R1	↑
				Q99MK8	Beta-adrenergic receptor kinase 1	ADRBK1	↑
				Q61011	Guanine nucleotide-binding protein G(I)/G(S)/G(T) subunit beta-3	GNB3	↓
Oxidative phosphorylation	2	0.035	0.3776	Q9D819	Inorganic pyrophosphatase	PPA1	↓
				Q9D0M3	Cytochrome c1	CYC1	↓
Cholinergic synapse	2	0.0317	0.3776	P21278	Guanine nucleotide-binding protein subunit alpha-11	GNA11	↓
				Q61011	Guanine nucleotide-binding protein G(I)/G(S)/G(T) subunit beta-3	GNB3	↓
Serotonergic synapse	2	0.0413	0.3776	P12023	Amyloid beta A4 protein	APP	↑
				Q61011	Guanine nucleotide-binding protein G(I)/G(S)/G(T) subunit beta-3	GNB3	↓
Medial prefrontal cortex							
Metabolic pathways	11	0.0284	0.2045	P56382	ATP synthase subunit epsilon	ATP5E	↑
				P12787	Cytochrome c oxidase subunit 5A	COX5A	↑
				P48758	Carbonyl reductase [NADPH] 1	CBR1	↓
				Q922Q4	Pyrroline-5-carboxylate reductase 2	PYCR2	↓
				Q99LB2	Dehydrogenase/reductase SDR family member 4	DHRS4	↓
				Q91VR2	ATP synthase subunit gamma	ATP5C1	↓
				O70250	Phosphoglycerate mutase 2	PGAM2	↓
				Q91XF0	Pyridoxine-5-phosphate oxidase	PNPO	↓
				Q80XN0	D-beta-hydroxybutyrate dehydrogenase	BDH1	↓
				Q99LS3	Phosphoserine phosphatase	PSPH	↓
				Q9DCC4	Pyrroline-5-carboxylate reductase 3	PYCRL	↓
Parkinson's disease	5	0.0005	0.0164	Q8CGK7	Guanine nucleotide-binding protein G(olf) subunit alpha	GNAL	↑
				P56382	ATP synthase subunit epsilon	ATP5E	↑
				P12787	Cytochrome c oxidase subunit 5A	COX5A	↑
				Q60930	Voltage-dependent anion-selective channel protein 2	VDAC2	↓
				Q91VR2	ATP synthase subunit gamma	ATP5C1	↓
Ribosome	5	0.0007	0.0164	Q9D1P0	39S ribosomal protein L13	MRPL13	↑
				P62908	40S ribosomal protein S3	RPS3	↓
				P62754	40S ribosomal protein S6	RPS6	↓
				P12970	60S ribosomal protein L7a	RPL7A	↓
				P84099	60S ribosomal protein L19	RPL19	↓
Alzheimer's disease	4	0.009	0.1298	P56382	ATP synthase subunit epsilon	ATP5E	↑
				P12787	Cytochrome c oxidase subunit 5A	COX5A	↑
				Q91VR2	ATP synthase subunit gamma	ATP5C1	↓
				P49615	Cyclin-dependent-like kinase 5	CDK5	↓
Biosynthesis of amino acids	4	0.0005	0.0164	O70250	Phosphoglycerate mutase 2	PGAM2	↓
				Q922Q4	Pyrroline-5-carboxylate reductase 2	PYCR2	↓
				Q99LS3	Phosphoserine phosphatase	PSPH	↓
				Q9DCC4	Pyrroline-5-carboxylate reductase 3	PYCRL	↓
Striatum							
Metabolic pathways	5	0.0004	0.0067	P12787	Cytochrome c oxidase subunit 5A	COX5A	↑
				P99028	Cytochrome b-c1 complex subunit 6	UQCRH	↑
				Q91XF0	Pyridoxine-5-phosphate oxidase	PNPO	↑

(*Continued*)

Table 2
(*Continued*)

Pathway	Proteins number	p	Corrected p	Accession number	Protein names	Gene names	Proteins expression
				P10518	Delta-aminolevulinic acid dehydratase	ALAD	↑
				Q9D020	Cytosolic 5-nucleotidase 3A	NT5C3A	↓
Alzheimer's disease	2	0.0044	0.0122	P12787	Cytochrome c oxidase subunit 5A	COX5A	↑
				P99028	Cytochrome b-c1 complex subunit 6	UQCRH	↑
Oxidative phosphorylation	2	0.0025	0.0121	P12787	Cytochrome c oxidase subunit 5A	COX5A	↑
				P99028	Cytochrome b-c1 complex subunit 6	UQCRH	↑
Parkinson's disease	2	0.0028	0.0121	P12787	Cytochrome c oxidase subunit 5A	COX5A	↑
				P99028	Cytochrome b-c1 complex subunit 6	UQCRH	↑
Huntington's disease	2	0.005	0.0122	P12787	Cytochrome c oxidase subunit 5A	COX5A	↑
				P99028	Cytochrome b-c1 complex subunit 6	UQCRH	↑

groups for each brain region (Fig. 3). In the hippocampus, two proteins (0.8%) overlapped between Tg-ctrl versus WT-ctrl and Tg-TRF versus Tg-PO groups: amyloid beta A4 protein (APP) and receptor-type tyrosine-protein phosphatase alpha (PTPRA). There was no overlap in mPFC and striatum. APP and PTPRA proteins were significantly increased ($p < 0.05$) in Tg-ctrl group compared with WT-ctrl (Fig. 3). In contrast, these proteins were significantly decreased ($p < 0.05$) in Tg-TRF group compared with Tg-PO (Fig. 3).

Pathway analysis

Pathway analysis based on the KEGG reference pathway databases (http://www.genome.jp/kegg/pathway.html) revealed that most of the significantly altered proteins between Tg-ctrl versus WT-ctrl mice hippocampus (Table 2) were involved in AD, oxidative phosphorylation, glutamatergic, cholinergic, and serotonergic synapse pathways. In mPFC (Table 2), the altered proteins between Tg-ctrl versus WT-ctrl participated in metabolic pathways, Parkinson's disease, ribosome, AD, and biosynthesis of amino acids. Meanwhile, in the striatum (Table 2), the altered proteins between Tg-ctrl versus WT-ctrl groups were engaged in metabolic pathways, AD, oxidative phosphorylation, Parkinson's disease, and Huntington's disease.

Pathway analysis of the altered proteins between Tg-TRF versus Tg-PO mice hippocampus (Table 3) showed that TRF modulated proteins were involved in metabolic pathways, Huntington's disease, AD, oxidative phosphorylation, and Parkinson's disease. In the mPFC (Table 3), the altered proteins between Tg-TRF and Tg-PO were engaged in metabolic pathways, biosynthesis of amino acids, carbon metabolism, AD, and arginine and proline

metabolism. Most of the significantly altered proteins between Tg-TRF and Tg-PO in the striatum (Table 3) participated in glycerolipid metabolism, glycolysis/gluconeogenesis, proteasome, valine, leucine and isoleucine degradation, and pentose and glucuronate interconversions.

DISCUSSION

The aim of the present study was to assess the effect of natural-source antioxidant treatment with tocotrienol-rich fraction (TRF) on the proteome profiles of AβPP/PS1 mice brains, by analyzing hippocampus, mPFC, and striatum. These regions were selected to represent areas of the brain known to be severely affected (hippocampus and mPFC) and moderately affected (striatum) in AD. According to the amyloid cascade hypothesis, abnormal aggregation of Aβ, including the formation of soluble oligomers and insoluble fibrils, leading to the formation of senile plaques, is an initial pathological alteration that leads to AD [31]. Previous studies have suggested that modulating Aβ aggregation and reducing brain Aβ aggregates would be beneficial as therapeutic targets against AD [32, 33]. However, amyloid burden and cognitive decline poorly correlate. There have been failures of recent clinical trials aimed at preventing cognitive decline by removing amyloid burden [34–36]. Proteomics studies still have a place for unravelling molecular mechanisms contributing to AD pathogenesis, and possibly finding new therapeutic strategies to combat the disease.

In this study, by comparing the proteome profiles of AβPP/PS1 mice (Tg-ctrl) with wild type (WT-ctrl) mice, we demonstrated alterations in levels of 43, 99, and 13 proteins in the AβPP/PS1 mice hippocampus, mPFC, and striatum, respectively (Table 1; Supplementary Table 3). Comparisons between the

Table 3

Kyoto Encyclopedia of Genes and Genomes (KEGG) pathway enrichment for the differentially expressed proteins from AβPP/PS1 transgenic mice treated with tocotrienol-rich fraction (Tg-TRF) compared with the vehicle control group, AβPP/PS1 transgenic mice treated with palm oil stripped of vitamin E (Tg-PO) using KOBAS. The pathways are arranged according to the number of differentially expressed proteins in each pathway. Only the top five enriched pathways ($p < 0.05$) are listed. ↓ represents significantly downregulated ($p < 0.05$) protein. ↑ represents significantly upregulated ($p < 0.05$) protein

Pathway	Proteins number	p	Corrected p	Accession number	Protein names	Gene names	Proteins expression
Hippocampus							
Metabolic pathways	25	0.0004	0.0099	P05064	Fructose-bisphosphate aldolase	ALDOA	↓
				P03911	NADH-ubiquinone oxidoreductase chain 4	MTND4	↓
				Q9Z0J4	Nitric oxide synthase, brain	NOS1	↓
				Q91YT0	NADH dehydrogenase [ubiquinone] flavoprotein 1	NDUFV1	↑
				Q8CGC7	Bifunctional glutamate/proline—tRNA ligase	EPRS	↓
				Q80UP3	Diacylglycerol kinase zeta	DGKZ	↓
				P62814	V-type proton ATPase subunit B, brain isoform	ATP6V1B2	↑
				Q61753	D-3-phosphoglycerate dehydrogenase	PHGDH	↑
				Q9Z1B3	1-phosphatidylinositol 4,5-bisphosphate phosphodiesterase beta-1	PLCB1	↓
				Q9CZS1	Aldehyde dehydrogenase X	ALDH1B1	↑
				Q91WD5	NADH dehydrogenase [ubiquinone] iron-sulfur protein 2	NDUFS2	↑
				Q7TMF3	NADH dehydrogenase [ubiquinone] 1 alpha subcomplex subunit 12	NDUFA12	↑
				Q91YQ5	Dolichyl-diphosphooligosaccharide—protein glycosyltransferase subunit 1	RPN1	↓
				P00397	Cytochrome c oxidase subunit 1	MTCO1	↓
				Q5SUR0	Phosphoribosylformylglycinamidine synthase	PFAS	↓
				Q91V92	ATP-citrate synthase	ACLY	↓
				Q920P5	Adenylate kinase isoenzyme 5	AK5	↑
				P56480	ATP synthase subunit beta	ATP5B	↑
				Q9CQ60	6-phosphogluconolactonase	PGLS	↑
				Q9DCS9	NADH dehydrogenase [ubiquinone] 1 beta subcomplex subunit 10	NDUFB10	↑
				Q924M7	Mannose-6-phosphate isomerase	MPI	↑
				P24549	Retinal dehydrogenase 1	ALDH1A1	↑
				P61922	4-aminobutyrate aminotransferase	ABAT	↑
				P26443	Glutamate dehydrogenase 1	GLUD1	↑
				Q4KWH5	1-phosphatidylinositol 4,5-bisphosphate phosphodiesterase eta-2	PLCH2	↓
Huntington's disease	12	3.99E-07	6.26E-05	P00397	Cytochrome c oxidase subunit 1	MTCO1	↓
				Q9DCS9	NADH dehydrogenase [ubiquinone] 1 beta subcomplex subunit 10	NDUFB10	↑
				Q9Z1B3	1-phosphatidylinositol 4,5-bisphosphate phosphodiesterase beta-1	PLCB1	↓
				Q91WD5	NADH dehydrogenase [ubiquinone] iron-sulfur protein 2	NDUFS2	↑
				Q91YT0	NADH dehydrogenase [ubiquinone] flavoprotein 1	NDUFV1	↑
				P11352	Glutathione peroxidase 1	GPX1	↓

(*Continued*)

Table 3
(*Continued*)

Pathway	Proteins number	*p*	Corrected *p*	Accession number	Protein names	Gene names	Proteins expression
				Q7TMF3	NADH dehydrogenase [ubiquinone] 1 alpha subcomplex subunit 12	NDUFA12	↑
				Q62108	Disks large homolog 4	DLG4	↓
				P56480	ATP synthase subunit beta	ATP5B	↑
				Q3UVX5	Metabotropic glutamate receptor 5	GRM5	↓
				O08788	Dynactin subunit 1	DCTN1	↓
				Q60931	Voltage-dependent anion-selective channel protein 3	VDAC3	↑
Alzheimer's disease	9	5.88E-05	0.0023	P12023	Amyloid beta A4 protein	APP	↓
				P00397	Cytochrome c oxidase subunit 1	MTCO1	↓
				Q9DCS9	NADH dehydrogenase [ubiquinone] 1 beta subcomplex subunit 10	NDUFB10	↑
				Q9Z0J4	Nitric oxide synthase, brain	NOS1	↓
				Q9Z1B3	1-phosphatidylinositol 4,5-bisphosphate phosphodiesterase beta-1	PLCB1	↓
				Q91WD5	NADH dehydrogenase [ubiquinone] iron-sulfur protein 2	NDUFS2	↑
				Q91YT0	NADH dehydrogenase [ubiquinone] flavoprotein 1	NDUFV1	↑
				Q7TMF3	NADH dehydrogenase [ubiquinone] 1 alpha subcomplex subunit 12	NDUFA12	↑
				P56480	ATP synthase subunit beta	ATP5B	↑
Oxidative phosphorylation	8	4.62E-05	0.0023	P00397	Cytochrome c oxidase subunit 1	MTCO1	↓
				Q9DCS9	NADH dehydrogenase [ubiquinone] 1 beta subcomplex subunit 10	NDUFB10	↑
				P03911	NADH-ubiquinone oxidoreductase chain 4	MTND4	↓
				Q91WD5	NADH dehydrogenase [ubiquinone] iron-sulfur protein 2	NDUFS2	↑
				Q91YT0	NADH dehydrogenase [ubiquinone] flavoprotein 1	NDUFV1	↑
				Q7TMF3	NADH dehydrogenase [ubiquinone] 1 alpha subcomplex subunit 12	NDUFA12	↑
				P56480	ATP synthase subunit beta	ATP5B	↑
				P62814	V-type proton ATPase subunit B, brain isoform	ATP6V1B2	↑
Parkinson's disease	8	7.53E-05	0.0024	P00397	Cytochrome c oxidase subunit 1	MTCO1	↓
				Q9DCS9	NADH dehydrogenase [ubiquinone] 1 beta subcomplex subunit 10	NDUFB10	↑
				P03911	NADH-ubiquinone oxidoreductase chain 4	MTND4	↓
				Q60931	Voltage-dependent anion-selective channel protein 3	VDAC3	↑
				Q91WD5	NADH dehydrogenase [ubiquinone] iron-sulfur protein 2	NDUFS2	↑
				Q91YT0	NADH dehydrogenase [ubiquinone] flavoprotein 1	NDUFV1	↑
				Q7TMF3	NADH dehydrogenase [ubiquinone] 1 alpha subcomplex subunit 12	NDUFA12	↑
				P56480	ATP synthase subunit beta	ATP5B	↑
Medial prefrontal cortex							
Metabolic pathways	7	0.0018	0.0315	P30275	Creatine kinase U-type	CKMT1	↑

(*Continued*)

Table 3
(*Continued*)

Pathway	Proteins number	p	Corrected p	Accession number	Protein names	Gene names	Proteins expression
				Q9CQZ6	NADH dehydrogenase [ubiquinone] 1 beta subcomplex subunit 3	NDUFB3	↑
				Q8K183	Pyridoxal kinase	PDXK	↑
				P54071	Isocitrate dehydrogenase [NADP]	IDH2	↑
				P05202	Aspartate aminotransferase	GOT2	↑
				O35435	Dihydroorotate dehydrogenase (quinone)	DHODH	↓
				P16858	Glyceraldehyde-3-phosphate dehydrogenase	GAPDH	↓
Biosynthesis of amino acids	3	0.0002	0.0132	P05202	Aspartate aminotransferase	GOT2	↑
				P54071	Isocitrate dehydrogenase [NADP]	IDH2	↑
				P16858	Glyceraldehyde-3-phosphate dehydrogenase	GAPDH	↓
Carbon metabolism	3	0.0006	0.0138	P05202	Aspartate aminotransferase	GOT2	↑
				P54071	Isocitrate dehydrogenase [NADP]	IDH2	↑
				P16858	Glyceraldehyde-3-phosphate dehydrogenase	GAPDH	↓
Alzheimer's disease	2	0.0271	0.1603	Q9CQZ6	NADH dehydrogenase [ubiquinone] 1 beta subcomplex subunit 3	NDUFB3	↑
				P16858	Glyceraldehyde-3-phosphate dehydrogenase	GAPDH	↓
Arginine and proline metabolism	2	0.0029	0.0407	P05202	Aspartate aminotransferase	GOT2	↑
				P30275	Creatine kinase U-type	CKMT1	↑
Striatum							
Glycerolipid metabolism	2	0.0027	0.0275	Q9JII6	Alcohol dehydrogenase [NADP(+)]	AKR1A1	↑
				Q9CZS1	Aldehyde dehydrogenase X	ALDH1B1	↑
Glycolysis/Gluconeogenesis	2	0.0035	0.0290	Q9JII6	Alcohol dehydrogenase [NADP(+)]	AKR1A1	↑
				Q9CZS1	Aldehyde dehydrogenase X	ALDH1B1	↑
Proteasome	2	0.0016	0.0265	Q9WVJ2	26S proteasome non-ATPase regulatory subunit 13	PSMD13	↑
				O55234	Proteasome subunit beta type-5	PSMB5	↑
Valine, leucine and isoleucine degradation	2	0.0019	0.0265	Q9CZS1	Aldehyde dehydrogenase X	ALDH1B1	↑
				P38060	Hydroxymethylglutaryl-CoA lyase	HMGCL	↑
Pentose and glucuronate interconversions	2	0.0008	0.0265	Q9JII6	Alcohol dehydrogenase [NADP(+)]	AKR1A1	↑
				Q9CZS1	Aldehyde dehydrogenase X	ALDH1B1	↑

AβPP/PS1 mice that received TRF (Tg-TRF) with the vehicle control group that received palm oil stripped of vitamin E (Tg-PO) showed 203, 29, and 23 proteins were altered in the hippocampus, mPFC, and striatum, separately (Table 1; Supplementary Table 4). The altered proteins in both comparisons were visualized in a Venn diagram to identify the overlapping proteins between groups in each studied brain region. We found that only two proteins: amyloid beta A4 protein (APP) and receptor-type tyrosine-protein phosphatase alpha (PTPRA), overlapped between both comparisons and showed a higher expression in AβPP/PS1 mice hippocampus compared with the WT mice (Fig. 3). The current study used double transgenic mice APP/PS1dE9, which expressed a chimeric mouse/human AβPP isoform 695 (line C3-3) driven by the mouse prion promoter, with a Swedish mutation in the AβPP sequence, that leads to increased total Aβ generation [22, 37]. These mice also expressed human PSEN1 lacking of exon 9 (line S-9), which represented the AD-associated mutation with exon 9 deletion [38]. Therefore, it is expected to find an increased level of APP protein in the AβPP/PS1
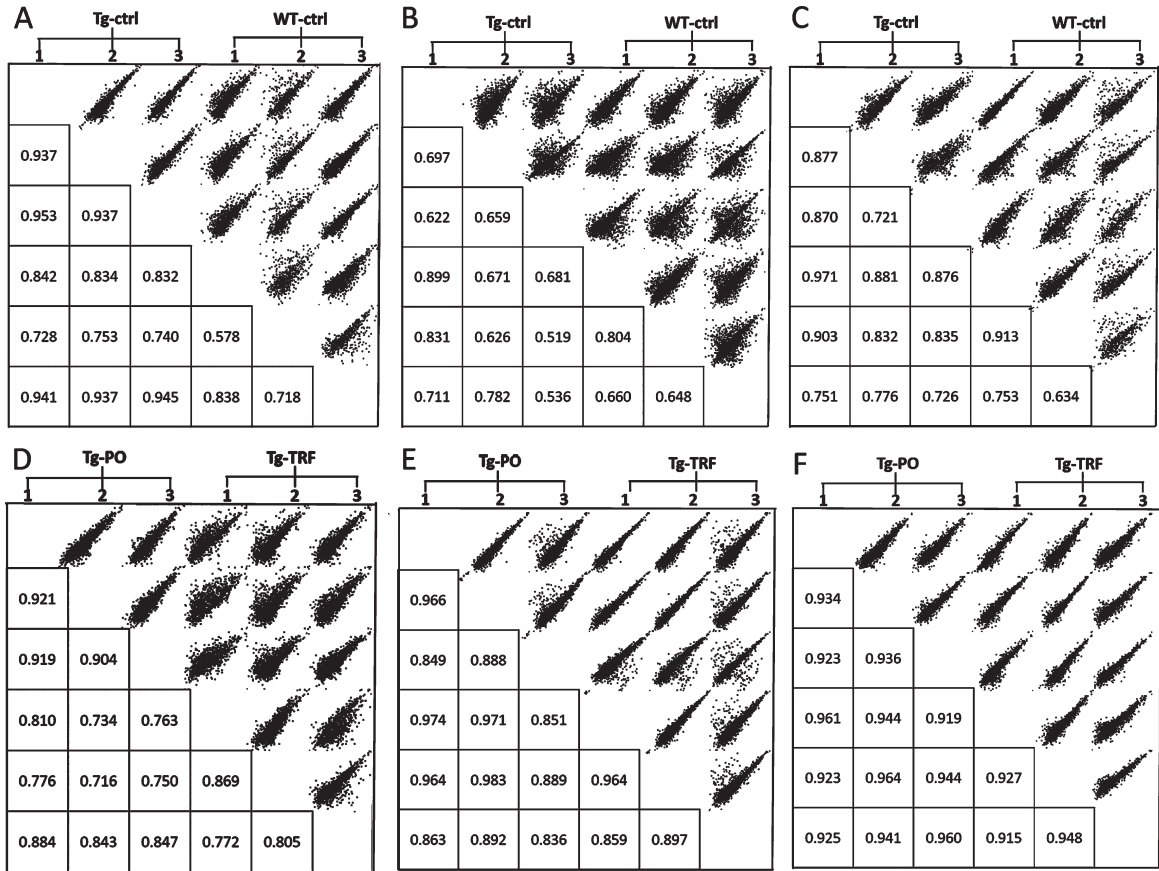
Fig. 1. Multi-scatter plots with Pearson correlation values of 0.5–1.0 suggest a good correlation between data obtained from the different experimental groups and biological replicates in the AβPP/PS1 mice without supplementation (Tg-ctrl) and wild-type mice (WT-ctrl) in the (A) hippocampus, (B) medial prefrontal cortex, and (C) striatum, as well as in the AβPP/PS1 mice received tocotrienol-rich fraction (Tg-TRF) and AβPP/PS1 mice received palm oil stripped of vitamin E (Tg-PO) groups in the (D) hippocampus, (E) medial prefrontal cortex, and (F) striatum.

mice hippocampus. Notably, the expression of these proteins was decreased in the AβPP/PS1 mice supplemented with TRF (Fig. 3). This finding concurred with our previous study which demonstrated that TRF modulated amyloid pathology by inhibiting Aβ fibril and oligomer formation *in vitro*, and also reduced Aβ deposition in AβPP/PS1 mice brain, particularly in the hippocampus and cortex [17]. Unfortunately, we cannot explain in detail how TRF was able to modulate this protein in the current untargeted proteomics analysis. Whether TRF is affecting APP levels, or APP metabolism to Aβ, or affecting steady-state levels of Aβ warrants further investigation. In our earlier study, we performed enzyme-linked immunosorbent assay (ELISA) and found that the levels of both $A\beta_{40}$ and $A\beta_{42}$ in hippocampus and cortex of AβPP/PS1 mice were not affected by TRF [17]. We also conducted metabolomics analysis

to understand the possible molecular mechanisms underlying this process and found that TRF was able to exhibit its potential therapeutic effects by modulating several metabolic pathways such as bioenergetics, neurotransmission, membrane lipid metabolism, and oxidative stress defense [18].

Other than APP protein, PTPRA level was also increased ($p < 0.05$) in the AβPP/PS1 mice hippocampus, and decreased with TRF supplementation (Fig. 3). Several studies have reported the importance of PTPRA in learning and memory, and this protein has been considered as a key mediator of neuronal migration and synaptic plasticity [39, 40]. The potential therapeutic target of tyrosine-protein phosphatase in various diseases including neuroinflammatory diseases has been reported [41–43]. PTPRA plays a central role as an activator of Src family kinases [44]. Src family kinases are a group
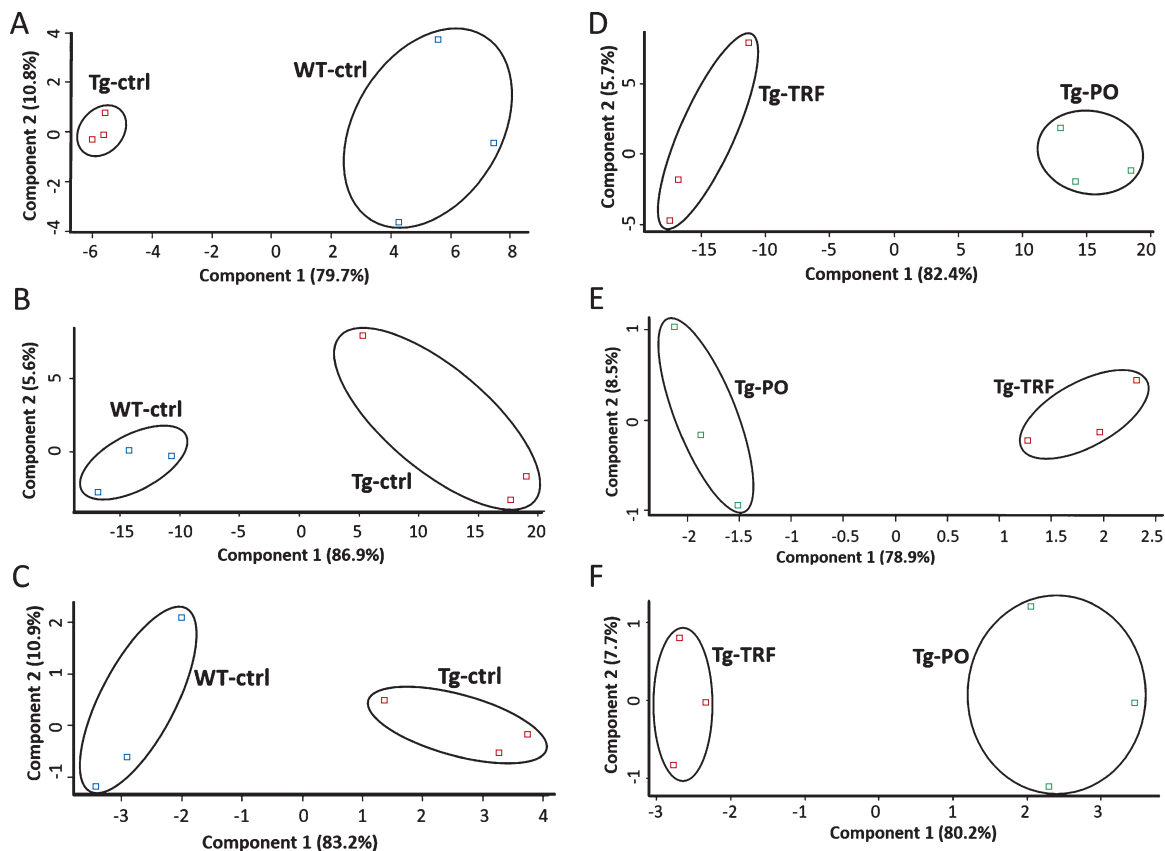
Fig. 2. Principal component analysis (PCA) plots of the proteomics data reveals replicates for each of the experimental group are closely clustered, suggesting high consistency between replicates in the AβPP/PS1 mice without supplementation (Tg-ctrl) and wild-type mice (WT-ctrl) in the (A) hippocampus, (B) medial prefrontal cortex, and (C) striatum, as well as in the AβPP/PS1 mice received tocotrienol-rich fraction (Tg-TRF) and AβPP/PS1 mice received palm oil stripped of vitamin E (Tg-PO) groups in the (D) hippocampus, (E) medial prefrontal cortex, and (F) striatum.

of genes that encode for nonreceptor protein kinases involved in cell growth regulation. c-Src, a product of Src family kinases is highly expressed in the brain [45]. However, overexpressed or highly activated c-Src causes uncontrolled cell proliferation, leading to various cancers in human [46, 47]. In addition, c-Src activation has also considered a key contributor to glutamate-induced neurodegeneration [48]. Thus, TRF may exert its neuroprotective effect by reducing the increased level of PTPRA in AβPP/PS1 mice hippocampus. Even though the exact mechanism is currently unclear, a previous study has demonstrated the neuroprotective mechanism of tocotrienol by suppressing glutamate-induced early activation of the c-Src kinase at nanomolar concentrations, thereby, preventing neuronal cell death [10]. Consistent with this, it was found in another study that tocotrienol inhibited the activation of c-Src and extracellular signal-regulated protein kinase (ERK)

in the mitogen-activated protein kinase (MAPK) cell signaling pathway for neuronal death, resulting in improved cognitive impairment in aged rats [49].

Aβ may not be the only player driving the cognitive decline in AD. Microtubule associated protein tau (MAPT) has also been considered a contributor to the onset of AD, leading to neuropathological conditions such as selective neuronal death, synaptic loss, and deposition of abnormal proteins including Aβ plaques and neurofibrillary tangles. MAPT was identified in these mice brains in the present study, yet the expression of this protein was unchanged. The AβPP/PS1 mouse is a transgenic mouse model that only develops amyloid deposits. It is a model system and fails to meet all criteria of AD human neuropathology such as formation of phosphorylated tau enriched neurofibrillary tangles [50, 51]. In order to understand the effect of TRF on both amyloid and
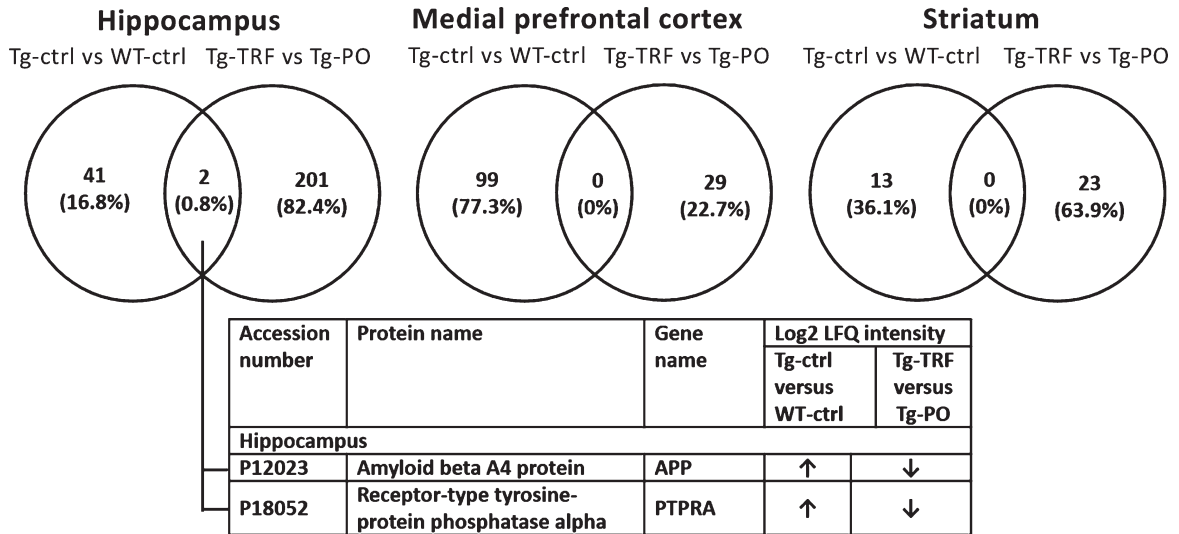
Hippocampus
Tg-ctrl vs WT-ctrl Tg-TRF vs Tg-PO

Medial prefrontal cortex
Tg-ctrl vs WT-ctrl Tg-TRF vs Tg-PO

Striatum
Tg-ctrl vs WT-ctrl Tg-TRF vs Tg-PO

| 41 (16.8%) | 2 (0.8%) | 201 (82.4%) | 99 (77.3%) | 0 (0%) | 29 (22.7%) | 13 (36.1%) | 0 (0%) | 23 (63.9%) |

Accession number	Protein name	Gene name	Log2 LFQ intensity	
			Tg-ctrl versus WT-ctrl	Tg-TRF versus Tg-PO
Hippocampus				
P12023	Amyloid beta A4 protein	APP	↑	↓
P18052	Receptor-type tyrosine-protein phosphatase alpha	PTPRA	↑	↓

Fig. 3. Venn diagram for differentially expressed proteins between groups in AβPP/PS1 mice without supplementation (Tg-ctrl) versus wild-type mice (WT-ctrl) and AβPP/PS1 mice received tocotrienol-rich fraction (Tg-TRF) versus AβPP/PS1 mice received palm oil stripped of vitamin E (Tg-PO) groups in hippocampus, medial prefrontal cortex, and striatum. The overlapped proteins between the groups were listed in the table below the diagram.

tau pathologies in the mouse brain, a further study is necessary by using different mouse models such as triple transgenic mouse (3×TgAD) which carries *APP*, *PSEN*, and *MAPT* mutations [52].

Neuroinflammation, an innate immunological response of the nervous system is also considered a hallmark of neurodegenerative diseases [53]. Microglia and astrocytes are the major types of glial cells and predominant mediators of inflammation within the central nervous system (CNS). The microglial function is regulated by apolipoprotein E (*APOE*) among other factors. *APOE* protein level was not significantly different in the AβPP/PS1 mice control compared to WT mice (Supplementary Table 1). Furthermore, microglial activation and the release of inflammatory mediators such as nitric oxide, chemokines, interleukins, and cytokines are also among the pathological mechanisms underlying the progression of neurodegenerative diseases [54, 55]. In this study, we found increased glial fibrillary acidic protein (GFAP) and decreased interleukin enhancer-binding protein 2 (ILF2) levels in the AβPP/PS1 mice hippocampus (Supplementary Table 3). TRF supplementation was, however, unable to modulate these proteins. This finding was in line with our previous study using an immunohistochemistry approach, which reported that AβPP/PS1 mice exhibited higher Iba1-immunoreactivity in the hippocampus and cortex compared with WT mice, but no difference was observed in the TRF treated group

[17]. It seems that TRF supplementation on these mice has no effect on microglial activity.

Recently, proteome profiling in human AD brain has reported AD-related alterations in the expression of over 5,000 proteins across six different brain regions [56]. The study also highlighted four candidate genes, syntaxin binding protein 1 (STXBP1), collapsin response-mediator protein 1 (CRMP1), actin-related protein 10 homologue (ACTR10), and amphiphysin (AMPH), which might be key mediators of the protein expression response to AD [56]. STXBP1, CRMP1, and AMPH proteins were identified in all selected brain regions of mice used in our study, but were not significantly altered (Supplementary Tables 1 and 2). However, ACTR10 protein level was significantly decreased in the AβPP/PS1 mice hippocampus treated with TRF compared with Tg-PO group, which may be a positive effect (Supplementary Table 4). ACTR10 plays a central role in the prion propagation and clearance process, thereby, affecting prion susceptibility [57]. This protein has also been identified in the aging mouse hippocampus [58] and AD human brain [56].

Genome-wide association studies (GWAS) have reported a number of genes related to AD, including clusterin (CLU), ephrin type-A receptor 1 (EPHA1), phosphatidylinositol-binding clathrin assembly protein (PICALM), myc box-dependent-interacting protein 1 (BIN1), ATP binding cassette subfamily A member 7 (ABCA7), membrane-spanning

4-domains subfamily A (MS4A), complement receptor type 1 (CR1), myeloid cell surface antigen CD33 (CD33), and CD2-associated protein (CD2AP) [59–61]. We identified three proteins with these gene names from our analysis (CLU, PICALM, and BIN1), but these proteins were not significantly altered in any of the mice groups. We found decreased expression of ephrin type-A receptor 4 (EPHA4) in Tg-TRF group, which could be neuroprotective. This is supported by a previous study which demonstrated EPHA4 as a mediator for synaptic plasticity impairment induced by Aβ, and the blockade of EPHA4 activity through targeting its ligand-binding domain reversed the synaptic deficits in AβPP/PS1 mice [62].

Aβ accumulation is considered a key early event in AD pathophysiology. However, several pathophysiological events may occur earlier than Aβ peptides in AD pathogenesis, including alterations in oxidative stress, nitrosative stress, metabolism, mitochondria, and inflammation [63–67]. Thus, supplementation with a natural antioxidant (i.e., vitamin E) could be essential to protect the brain against these events. Vitamin E plays a central role in scavenging peroxyl radical, preventing lipid peroxidation, and protecting polyunsaturated fatty acids (PUFAs) and other cell membranes components and lipoproteins from oxidation by free radicals [68]. Tocotrienols in particular have been shown previously to exert antioxidative effect in *in vitro* and *in vivo* studies [69–71]. For instance, up to $100 \, \mu mol/L$ of γ-tocotrienol concentration protected against hydrogen peroxide (H_2O_2)-induced cell death and apoptosis in primary astrocyte cultures [69]. In addition, α-tocotrienol has been shown to protect neuronal cell from glutamate-induced toxicity primarily by a direct antioxidant action [70]. In an *in vivo* study, three months supplementation of TRF (200 mg/kg) has been reported to markedly reduce lipid peroxidation, modulate antioxidant enzymes activity and brain arginine metabolism, and also improve memory in aged rats [19, 71]. Tocotrienols supplementation has also been reported to improve lipid profiles in chronic hemodialysis patients [72]. In line with the previous findings, we also observed possible antioxidative mechanism of TRF in AβPP/PS1 mice brain, particularly hippocampus. The present study demonstrated decreased ($p < 0.05$) expression of proteins involved in oxidative phosphorylation such as inorganic pyrophosphatase (PPA1) and cytochrome c1 (CYC1) in the AβPP/PS1 mice hippocampus (Table 2). In contrast, six proteins involved in this pathway (Table 3) were increased ($p < 0.05$) with

TRF supplementation in these mice hippocampus: NADH dehydrogenase [ubiquinone] 1 beta subcomplex subunit 10 (NDUFB10), NADH dehydrogenase [ubiquinone] iron-sulfur protein 2 (NDUFS2), NADH dehydrogenase [ubiquinone] flavoprotein 1 (NDUFV1), NADH dehydrogenase [ubiquinone] 1 alpha subcomplex subunit 12 (NDUFA12), ATP synthase subunit beta (ATP5B), and V-type proton ATPase subunit B, brain isoform (ATP6V1B2). Oxidative stress and mitochondrial dysfunction have been recognized as among the most prominent features implicated in AD pathophysiology [73]. Previous studies have shown a correlation between the decreased expression of nuclear or mitochondrial genes in the neocortex of AD patients with progressive reductions in brain glucose metabolism [74, 75]. Deregulation of oxidative phosphorylation proteins was also observed in a triple transgenic mouse of AD [76]. Thus, the modulations of proteins expression involved in this pathway may be due to an antioxidative mechanism of TRF reducing oxidative stress in the AβPP/PS1 mice brain.

Overall, the present study provides insights into understanding the proteome changes in the hippocampus, mPFC, and striatum of AβPP/PS1 transgenic mice supplemented with TRF. Our proteomics analysis using liquid chromatography coupled to Q Exactive HF Orbitrap mass spectrometry demonstrated that the modulation of proteome profile by TRF could be due to its effect on Aβ, or independent of this, as illustrated in Fig. 4. For instance, the decreased level of APP in the AβPP/PS1 mice receiving TRF may be key to the reduced Aβ deposits and improved cognitive function [17]. In addition, the reduced level of PTPRA is possibly involved in the decreased activation of c-Src kinase, preventing glutamate-induced neurodegeneration and also contributes to the improved memory in the AβPP/PS1 mice. The mechanism of TRF in improving cognitive function may also possibly occur by modulating other proteins in metabolic pathways, AD, and oxidative phosphorylation. Altered metabolic pathways related to bioenergetics, neurotransmission, membrane lipid metabolism, and oxidative stress defense as reported in our previous metabolomics analysis may also lead to the improved memory in AβPP/PS1 mice [18] (Fig. 4).

Even though our proposed mechanism of TRF as illustrated in Fig. 4 is speculative at this moment, hopefully it can at least provide a general overview to understand the possible molecular mechanisms of TRF in ameliorating the cognitive deficits in
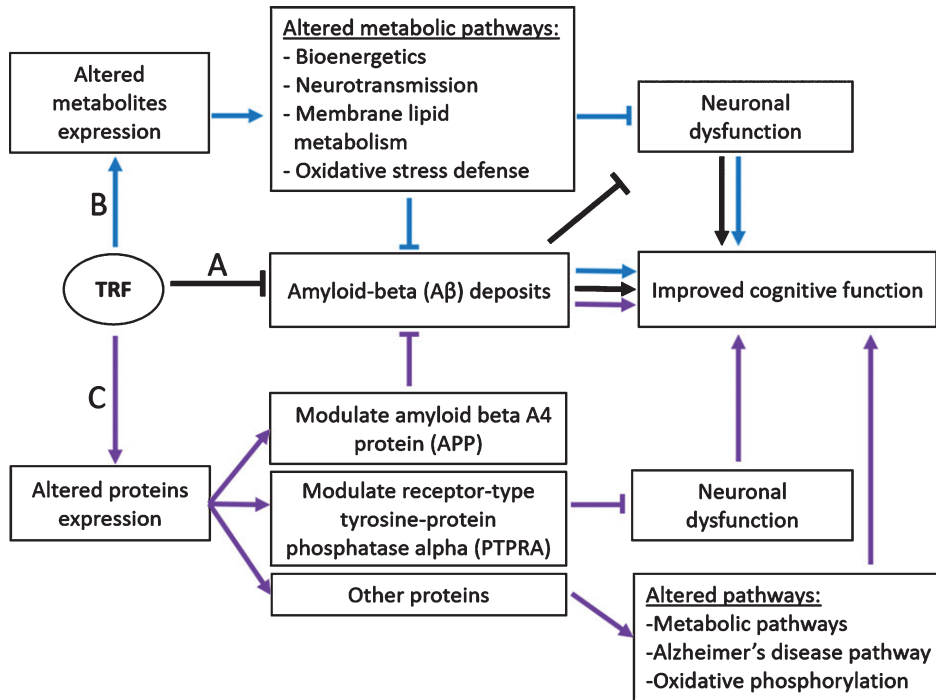
Fig. 4. Proposed mechanisms of TRF action in improving cognitive function in AβPP/PS1 mice. Aβ deposits, altered metabolites, and proteins expression cause neuronal dysfunction leading to cognitive impairment. A) TRF reduces Aβ deposition and improves cognitive function (black arrow) [17]. B) TRF modulates metabolic pathways, reducing neuronal dysfunction, and improves cognitive function (blue arrow) [18]. C) TRF modulates amyloid beta A4 protein (APP) leading to reduced Aβ deposits and improved cognitive function. TRF also modulates receptor-type tyrosine-protein phosphatase alpha (PTPRA), reducing neuronal dysfunction, and improves memory. TRF may also improve memory by modulating other proteins involved in metabolic pathways, Alzheimer's disease pathway, and oxidative phosphorylation (purple arrow). Figure modified from Durani et al. [18].

AβPP/PS1 mice. In future, further studies such as multi-omics integration approach or targeted proteomics and metabolomics can be implemented to understand the relationship between metabolites and proteins changes, and the exact molecular mechanisms for TRF to slow down AD progression. In addition, a study using AβPP/PS1 mice may open avenues to understand the mechanism of TRF in modulating amyloid pathology, but it is important to note that this animal model does not represent overall AD pathogenesis. Thus, the use of other transgenic mouse models such as triple transgenic mouse which carries *APP*, *PSEN*, and *MAPT* mutations, or 5×FAD mouse may be useful to confirm and enhance our understanding of AD pathogenesis.

In summary, TRF potentially exerts its neuroprotective effects in AβPP/PS1 mice brain by modulating proteins involved in various biochemical pathways including metabolic pathways, AD, and oxidative phosphorylation. Our current findings demonstrated that TRF supplementation altered proteins in the AβPP/PS1 mice brain in a region-specific manner. TRF also modulated APP and PTPRA protein expression in AβPP/PS1 mice hippocampus. However, whether the improved cognitive performance upon TRF treatment is associated with the changes in APP and PTPRA levels warrants further investigation.

SUPPLEMENTARY MATERIAL

The supplementary material is available in the electronic version of this article: http://dx.doi.org/10.3233/JAD-181171.

REFERENCES

[1] Selkoe DJ, Schenk D (2003) Alzheimer's disease: Molecular understanding predicts amyloid-based therapeutics. *Annu Rev Pharmacol Toxicol* **43**, 545-584.

[2] Chami L, Checler F (2012) BACE1 is at the crossroad of a toxic vicious cycle involving cellular stress and β-amyloid production in Alzheimer's disease. *Mol Neurodegener* **7**, 52.

[3] Povova J, Ambroz P, Bar M, Pavukova V, Sery O, Tomaskova H, Janout V (2012) Epidemiological of and risk factors for Alzheimer's disease: A review. *Biomed Pap Med Fac Univ Palacky Olomouc Czech Repub* **156**, 108-114.

[4] Cacace R, Sleegers K, Van Broeckhoven C (2016) Molecular genetics of early-onset Alzheimer's disease revisited. *Alzheimers Dement* **12**, 733-748.

[5] Lin MT, Beal MF (2006) Mitochondrial dysfunction and oxidative stress in neurodegenerative diseases. *Nature* **443**, 787-795.

[6] Dysken MW, Sano M, Asthana S, Vertrees JE, Pallaki M, Llorente M, Love S, Schellenberg GD, McCarten JR, Malphurs J, Prieto S, Chen P, Loreck DJ, Trapp G, Bakshi RS, Mintzer JE, Heidebrink JL, Vidal-Cardona A, Arroyo LM, Cruz AR, Zachariah S, Kowall NW, Chopra MP, Craft S, Thielke S, Turvey CL, Woodman C, Monnell KA, Gordon K, Tomaska J, Segal Y, Peduzzi PN, Guarino PD (2014) Effect of vitamin E and memantine on functional decline in Alzheimer disease: The TEAM-AD VA cooperative randomized trial. *JAMA* **311**, 33-44.

[7] Morris MC, Evans DA, Tangney CC, Bienias JL, Wilson RS, Aggarwal NT, Scherr PA (2005) Relation of the tocopherol forms to incident Alzheimer disease and to cognitive change. *Am J Clin Nutr* **81**, 508-514.

[8] Morris MC, Evans DA, Bienias JL, Tangney CC, Wilson RS (2002) Vitamin E and cognitive decline in older persons. *Arch Neurol* **59**, 1125-1132.

[9] Petersen RC, Thomas RG, Grundman M, Bennett D, Doody R, Ferris S, Galasko D, Jin S, Kaye J, Levey A, Pfeiffer E, Sano M, van Dyck CH, Thal LJ (2005) Vitamin E and donepezil for the treatment of mild cognitive impairment. *N Engl J Med* **352**, 2379-2388.

[10] Sen CK, Khanna S, Roy S, Packer L (2000) Molecular basis of vitamin E action. Tocotrienol potently inhibits glutamate-induced pp60(c-Src) kinase activation and death of HT4 neuronal cells. *J Biol Chem* **275**, 13049-13055.

[11] Kamal-Eldin A, Appelqvist LA (1996) The chemistry and antioxidant properties of tocopherols and tocotrienols. *Lipids* **31**, 671-701.

[12] Aggarwal BB, Sundaram C, Prasad S, Kannappan R (2010) Tocotrienols, the vitamin E of the 21st century: Its potential against cancer and other chronic diseases. *Biochem Pharmacol* **80**, 1613-1631.

[13] Suzuki YJ, Tsuchiya M, Wassall SR, Choo YM, Govil G, Kagan VE, Packer L (1993) Structural and dynamic membrane properties of alpha-tocopherol and alpha-tocotrienol: Implication to the molecular mechanism of their antioxidant potency. *Biochemistry* **32**, 10692-10699.

[14] Mangialasche F, Kivipelto M, Mecocci P, Rizzuto D, Palmer K, Winblad B, Fratiglioni L (2010) High plasma levels of vitamin E forms and reduced Alzheimer's disease risk in advanced age. *J Alzheimers Dis* **20**, 1029-1037.

[15] Sundram K, Sambanthamurthi R, Tan YA (2003) Palm fruit chemistry and nutrition. *Asia Pac J Clin Nutr* **12**, 355-362.

[16] Sen CK, Rink C, Khanna S (2010) Palm oil–derived natural vitamin E α-tocotrienol in brain health and disease. *J Am Coll Nutr* **29**, 314S-323S.

[17] Ibrahim NF, Yanagisawa D, Durani LW, Hamezah HS, Damanhuri HA, Wan Ngah WZ, Tsuji M, Kiuchi Y, Ono K, Tooyama I (2017) Tocotrienol-rich fraction modulates amyloid pathology and improves cognitive function in AβPP/PS1 mice. *J Alzheimers Dis* **55**, 597-612.

[18] Durani LW, Hamezah HS, Ibrahim NF, Yanagisawa D, Nasaruddin ML, Mori M, Azizan KA, Damanhuri HA, Makpol S, Wan Ngah WZ, Tooyama I (2018) Tocotrienol-rich fraction of palm oil improves behavioral impairments and regulates metabolic pathways in AβPP/PS1 mice. *J Alzheimers Dis* **64**, 249-267.

[19] Mazlan M, Hamezah HS, Taridi NM, Jing Y, Liu P, Zhang H, Wan Ngah WZ, Damanhuri HA (2017) Effects of aging and tocotrienol-rich fraction supplementation on brain arginine metabolism in rats. *Oxid Med Cell Longev* **2017**, 6019796.

[20] Khor SC, Wan Ngah WZ, Mohd Yusof YA, Abdul Karim N, Makpol S (2017) Tocotrienol-rich fraction ameliorates antioxidant defense mechanisms and improves replicative senescence-associated oxidative stress in human myoblasts. *Oxid Med Cell Longev* **2017**, 3868305.

[21] Rahman AA, Makpol S, Jamal R, Harun R, Mokhtar N, Ngah WZW (2014) Tocotrienol-rich fraction, [6]-gingerol and epigallocatechin gallate inhibit proliferation and induce apoptosis of glioma cancer cells. *Molecules* **19**, 14528-14541.

[22] Borchelt DR, Ratovitski T, Lare J Van, Lee MK, Gonzales V, Jenkins NA, Copeland NG, Price DL, Sisodia SS (1997) Accelerated amyloid deposition in the brains of transgenic mice coexpressing mutant presenilin 1 and amyloid precursor proteins. *Neuron* **19**, 939-945.

[23] Hamezah HS, Durani LW, Yanagisawa D, Ibrahim NF, Aizat WM, Bellier JP, Makpol S, Ngah WZW, Damanhuri HA, Tooyama I (2018) Proteome profiling in the hippocampus, medial prefrontal cortex, and striatum of aging rat. *Exp Gerontol* **111**, 53-64.

[24] Iovinella I, Caputo B, Michelucci E, Dani FR, della Torre A (2015) Candidate biomarkers for mosquito age-grading identified by label-free quantitative analysis of protein expression in Aedes albopictus females. *J Proteomics* **128**, 272-279.

[25] Tyanova S, Temu T, Cox J (2016) The MaxQuant computational platform for mass spectrometry-based shotgun proteomics. *Nat Protoc* **11**, 2301-2319.

[26] Vizcaíno JA, Côté RG, Csordas A, Dianes JA, Fabregat A, Foster JM, Griss J, Alpi E, Birim M, Contell J, O'Kelly G, Schoenegger A, Ovelleiro D, Pérez-Riverol Y, Reisinger F, Ríos D, Wang R, Hermjakob H (2013) The Proteomics Identifications (PRIDE) database and associated tools: Status in 2013. *Nucleic Acids Res* **41**, 1063-1069.

[27] Tyanova S, Temu T, Sinitcyn P, Carlson A, Hein MY, Geiger T, Mann M, Cox J (2016) The Perseus computational platform for comprehensive analysis of (prote)omics data. *Nat Methods* **13**, 731-740.

[28] Oliveros JC (2007) VENNY. An interactive tool for comparing lists with Venn diagrams. *BioinfoGP, CNB-CSIC*.

[29] Wu J, Mao X, Cai T, Luo J, Wei L (2006) KOBAS server: A web-based platform for automated annotation and pathway identification. *Nucleic Acids Res* **34**, W720-724.

[30] Xie C, Mao X, Huang J, Ding Y, Wu J, Dong S, Kong L, Gao G, Li C-Y, Wei L (2011) KOBAS 2.0: A web server for annotation and identification of enriched pathways and diseases. *Nucleic Acids Res* **39**, 316-322.

[31] Hardy J, Selkoe DJ (2002) The amyloid hypothesis of Alzheimer's disease: Progress and problems on the road to therapeutics. *Science* **297**, 353-356.

[32] Citron M (2010) Alzheimer's disease: Strategies for disease modification. *Nat Rev Drug Discov* **9**, 387-398.

[33] Haass C, Selkoe DJ (2007) Soluble protein oligomers in neurodegeneration: Lessons from the Alzheimer's amyloid beta-peptide. *Nat Rev Mol Cell Biol* **8**, 101-112.

[34] Selkoe DJ, Hardy J (2016) The amyloid hypothesis of Alzheimer's disease at 25 years. *EMBO Mol Med* **8**, 595-608.

[35] Becker RE, Greig NH (2008) Alzheimer's disease drug development in 2008 and beyond: Problems and opportunities. *Curr Alzheimer Res* **5**, 346-357.

[36] Giacobini E, Becker RE (2007) One hundred years after the discovery of Alzheimer's disease. A turning point for therapy? *J Alzheimers Dis* **12**, 37-52.

[37] Savonenko AV, Xu GM, Price DL, Borchelt DR, Markowska AL (2003) Normal cognitive behavior in two distinct congenic lines of transgenic mice hyperexpressing mutant APP SWE. *Neurobiol Dis* **12**, 194-211.

[38] Lee MK, Borchelt DR, Kim G, Thinakaran G, Slunt HH, Ratovitski T, Martin LJ, Kittur A, Gandy S, Levey AI, Jenkins N, Copeland N, Price DL, Sisodia SS (1997) Hyperaccumulation of FAD-linked presenilin 1 variants *in vivo*. *Nat Med* **3**, 756-760.

[39] Petrone A, Battaglia F, Wang C, Dusa A, Su J, Zagzag D, Bianchi R, Casaccia-Bonnefil P, Arancio O, Sap J (2003) Receptor protein tyrosine phosphatase alpha is essential for hippocampal neuronal migration and long-term potentiation. *EMBO J* **22**, 4121-4131.

[40] Lei G, Xue S, Che Á, Liu Q, Xu J, Kwan CL, Fu Y, Lu Y, Liu M, Harder KW, Yu X (2002) Gain control of N-methyl-D-aspartate receptor activity by receptor-like protein tyrosine phosphatase alpha. *EMBO J* **21**, 2977-2989.

[41] Verma S, Sharma S (2018) Protein tyrosine phosphatase as potential therapeutic target in various disorders. *Curr Mol Pharmacol* **11**, 191-202.

[42] Song GJ, Jung M, Kim J-H, Park H, Rahman MH, Zhang S, Zhang Z-Y, Park DH, Kook H, Lee I-K, Suk K (2016) A novel role for protein tyrosine phosphatase 1B as a positive regulator of neuroinflammation. *J Neuroinflammation* **13**, 86.

[43] He R, Yu Z, Zhang R, Zhang Z (2014) Protein tyrosine phosphatases as potential therapeutic targets. *Acta Pharmacol Sin* **35**, 1227-1246.

[44] Pallen CJ (2003) Protein tyrosine phosphatase alpha (PTPalpha): A Src family kinase activator and mediator of multiple biological effects. *Curr Top Med Chem* **3**, 821-835.

[45] Soriano P, Montgomery C, Geske R, Bradley A (1991) Targeted disruption of the c-src proto-oncogene leads to osteopetrosis in mice. *Cell* **64**, 693-702.

[46] Sen B, Johnson FM (2011) Regulation of Src family kinases in human cancers. *J Signal Transduct* **2011**, 865819.

[47] Ishizawar R, Parsons SJ (2004) c-Src and cooperating partners in human cancer. *Cancer Cell* **6**, 209-214.

[48] Khanna S, Roy S, Park H-A, Sen CK (2007) Regulation of c-Src activity in glutamate-induced neurodegeneration. *J Biol Chem* **282**, 23482-23490.

[49] Kaneai N, Sumitani K, Fukui K, Koike T, Takatsu H, Urano S (2016) Tocotrienol improves learning and memory deficit of aged rats. *J Clin Biochem Nutr* **58**, 114-121.

[50] Jankowsky JL, Zheng H (2017) Practical considerations for choosing a mouse model of Alzheimer's disease. *Mol Neurodegener* **12**, 89.

[51] Duyckaerts C, Potier M-C, Delatour B (2008) Alzheimer disease models and human neuropathology: Similarities and differences. *Acta Neuropathol* **115**, 5-38.

[52] Oddo S, Caccamo A, Shepherd JD, Murphy MP, Golde TE, Kayed R, Metherate R, Mattson MP, Akbari Y, LaFerla FM (2003) Triple-transgenic model of Alzheimer's disease with plaques and tangles: Intracellular Abeta and synaptic dysfunction. *Neuron* **39**, 409-421.

[53] Heneka MT, Carson MJ, Khoury J El, Gary E, Brosseron F, Feinstein DL, Jacobs AH, Wyss-coray T, Vitorica J, Ransohoff RM (2018) Neuroinflammation in Alzheimer's disease. *Lancet Neurol* **14**, 388-405.

[54] Frank-Cannon TC, Alto LT, McAlpine FE, Tansey MG (2009) Does neuroinflammation fan the flame in neurodegenerative diseases? *Mol Neurodegener* **4**, 47.

[55] Morales I, Guzmán-Martínez L, Cerda-Troncoso C, Farías GA, Maccioni RB (2014) Neuroinflammation in the pathogenesis of Alzheimer's disease. A rational framework for the search of novel therapeutic approaches. *Front Cell Neurosci* **8**, 112.

[56] Xu J, Patassini S, Rustogi N, Riba-Garcia I, Hale BD, Phillips AM, Waldvogel H, Haines R, Bradbury P, Stevens A, Faull RLM, Dowsey AW, Cooper GJS, Unwin RD (2019) Regional protein expression in human Alzheimer's brain correlates with disease severity. *Commun Biol* **2**, 43.

[57] Brown CA, Schmidt C, Poulter M, Hummerich H, Klohn P, Jat P, Mead S, Collinge J, Lloyd SE (2014) *In vitro* screen of prion disease susceptibility genes using the scrapie cell assay. *Hum Mol Genet* **23**, 5102-5108.

[58] Dempsey KM, Ali HH (2014) Identifying aging-related genes in mouse hippocampus using gateway nodes. *BMC Syst Biol* **8**, 1-16.

[59] Bettens K, Sleegers K, Van Broeckhoven C (2013) Genetic insights in Alzheimer's disease. *Lancet Neurol* **12**, 92-104.

[60] Karch CM, Goate AM (2015) Alzheimer's disease risk genes and mechanisms of disease pathogenesis. *Biol Psychiatry* **77**, 43-51.

[61] Morgan K (2011) The three new pathways leading to Alzheimer's disease. *Neuropathol Appl Neurobiol* **37**, 353-357.

[62] Fu AKY, Hung K-W, Huang H, Gu S, Shen Y, Cheng EYL, Ip FCF, Huang X, Fu W-Y, Ip NY (2014) Blockade of EphA4 signaling ameliorates hippocampal synaptic dysfunctions in mouse models of Alzheimer's disease. *Proc Natl Acad Sci U S A* **111**, 9959-9964.

[63] Sperling RA, Aisen PS, Beckett LA, Bennett DA, Craft S, Fagan AM, Iwatsubo T, Jack CRJ, Kaye J, Montine TJ, Park DC, Reiman EM, Rowe CC, Siemers E, Stern Y, Yaffe K, Carrillo MC, Thies B, Morrison-Bogorad M, Wagster M V, Phelps CH (2011) Toward defining the preclinical stages of Alzheimer's disease: Recommendations from the National Institute on Aging-Alzheimer's Association workgroups on diagnostic guidelines for Alzheimer's disease. *Alzheimers Dement* **7**, 280-292.

[64] Pimplikar SW, Nixon RA, Robakis NK, Shen J, Tsai L-H (2010) Amyloid-independent mechanisms in Alzheimer's disease pathogenesis. *J Neurosci* **30**, 14946-14954.

[65] Mangialasche F, Polidori MC, Monastero R, Ercolani S, Camarda C, Cecchetti R, Mecocci P (2009) Biomarkers of oxidative and nitrosative damage in Alzheimer's disease and mild cognitive impairment. *Ageing Res Rev* **8**, 285-305.

[66] Sayre LM, Perry G, Smith MA (2008) Oxidative stress and neurotoxicity. *Chem Res Toxicol* **21**, 172-188.

[67] Wyss-Coray T (2006) Inflammation in Alzheimer disease: Driving force, bystander or beneficial response? *Nat Med* **12**, 1005-1015.

[68] Galli F, Azzi A, Birringer M, Cook-Mills JM, Eggersdorfer M, Frank J, Cruciani G, Lorkowski S, Ozer NK (2017) Vitamin E: Emerging aspects and new directions. *Free Radic Biol Med* **102**, 16-36.

[69] Mazlan M, Sue Mian T, Mat Top G, Zurinah Wan Ngah W (2006) Comparative effects of alpha-tocopherol and gamma-tocotrienol against hydrogen peroxide induced apoptosis on primary-cultured astrocytes. *J Neurol Sci* **243**, 5-12.

[70] Saito Y, Nishio K, Akazawa YO, Yamanaka K, Miyama A, Yoshida Y, Noguchi N, Niki E (2010) Cytoprotective effects of vitamin E homologues against glutamate-induced cell death in immature primary cortical neuron cultures: Tocopherols and tocotrienols exert similar effects by antioxidant function. *Free Radic Biol Med* **49**, 1542-1549.

[71] Taridi NM, Abd Rani N, Abd Latiff A, Ngah WZW, Mazlan M (2014) Tocotrienol rich fraction reverses age-related deficits in spatial learning and memory in aged rats. *Lipids* **49**, 855-869.

[72] Daud ZAM, Tubie B, Sheyman M, Osia R, Adams J, Tubie S, Khosla P (2013) Vitamin E tocotrienol supplementation improves lipid profiles in chronic hemodialysis patients. *Vasc Health Risk Manag* **9**, 747-761.

[73] Wang X, Wang W, Li L, Perry G, Lee H, Zhu X (2014) Oxidative stress and mitochondrial dysfunction in Alzheimer's disease. *Biochim Biophys Acta* **1842**, 1240-1247.

[74] Chandrasekaran K, Hatanpaa K, Brady DR, Rapoport SI (1996) Evidence for physiological down-regulation of brain oxidative phosphorylation in Alzheimer's disease. *Exp Neurol* **142**, 80-88.

[75] Chandrasekaran K, Hatanpaa K, Rapoport SI, Brady DR (1997) Decreased expression of nuclear and mitochondrial DNA-encoded genes of oxidative phosphorylation in association neocortex in Alzheimer disease. *Brain Res Mol Brain Res* **44**, 99-104.

[76] Rhein V, Song X, Wiesner A, Ittner LM, Baysang G, Meier F, Ozmen L, Bluethmann H, Drose S, Brandt U, Savaskan E, Czech C, Gotz J, Eckert A (2009) Amyloid-beta and tau synergistically impair the oxidative phosphorylation system in triple transgenic Alzheimer's disease mice. *Proc Natl Acad Sci U S A* **106**, 20057-20062.